

# Neighborhood designs for low-density social housing energy efficiency: Case study of an arid city in Argentina

María Belén Sosa\*, Erica Norma Correa, María Alicia Cantón

Instituto de Ambiente, Hábitat y Energía (INAHE) - Consejo Nacional de Investigaciones Científicas y Técnicas (CONICET) - CCT-Mendoza, Av. Ruiz Leal s/n - Parque Gral. San Martín (5500), Mendoza, Argentina

## ARTICLE INFO

### Article history:

Received 19 December 2017

Revised 20 February 2018

Accepted 2 March 2018

Available online 12 March 2018

### Keywords:

Urban form

Neighborhood design

Residential energy consumption

Heat island effect

Arid cities

## ABSTRACT

Neighborhood planning and design strategies that reduce outdoor air temperatures would improve the thermal and energy performance of cities in arid regions. This study presents the thermal behavior and energy consumption of different urban scenarios for low-density social housing neighborhoods in Mendoza, Argentina. The microclimates of three representative urban canyons located in three different social housing neighborhoods were monitored. These neighborhoods have different layouts but share other similar features, which allow the behavior of their microclimates to be compared. Thus, 48 simulations were conducted using ENVI-met software to test neighborhood-level scenarios with the following features: two street widths (16 and 20 m), three layout grids (multi-azimuthal, Cul-de-Sac, and rectangular), and four street orientations (E-W, N-S, NE-SW, and NW-SE). The energy consumption of each urban scenario was then estimated and compared. The results show that, in a house constructed without following bioclimatic design strategies, at least 21% of the auxiliary energy required to achieve a comfortable indoor temperature (25 °C) during summer can be saved. Energy savings depend on a suitable layout and street orientation, urban trees, and the albedo of the building materials. This study highlights the importance of planning and design decisions, especially for social housing settlements in arid cities.

© 2018 Elsevier B.V. All rights reserved.

## 1. Introduction

By 2030, the global energy demand is expected to grow by 40–50% [52]. Providing electricity to the global population would require an annual investment of \$52 billion per year by 2030, which exceeds twice the level mobilized under current and planned policies [12]. Energy usage in residential buildings accounts for a significant portion of global energy consumption. The U.S. Energy Information Administration estimates that the country's electricity usage in 2016 exceeded that in 1950 by more than 13-fold, and space cooling by the residential sector (i.e., air conditioning) accounted for the highest electricity consumptions [9].

The amount of energy used by the residential sector depends on the climate, building characteristics, the number and characteristics of energy-consuming devices, and the inhabitants' socioeconomic level [5,36]. Cities in arid zones must survive in an environment that is characterized by extreme climatic conditions, with high solar radiation and air temperatures. In this climate, the urban

heat island (UHI) effect and warming are most noticeable during the summer and affect energy consumption via air conditioning as well as the health of city dwellers.

The main causes of these phenomena are the modification of land surfaces and waste heat generated by energy usage [24,44]. Regarding energy consumption, Lin et al. [25] determined that a 1 °C increase in temperature increases peak electricity demand by 2–4%, and Salamanca et al. [40] demonstrated that extended use of air conditioning increases the air temperature of arid cities by 1 °C at night. As outdoor temperatures rise, more energy will be required for cooling system operation. Increased energy demand will increase its price, rendering it unaffordable to low-income households. This generates a cycle that negatively affects urban sustainability [56]. The high cost of energy will detriment the indoor habitability of social housing [4]. Therefore, designing energy efficient dwellings will reduce electricity bills for residents [34].

One of the most important aspects of urban planning is the creation of sustainable urban environments. The planning process is closely related to the climate [57]. The LEED-ND rating system recommends that an energy-efficient building is good, but an energy-efficient neighborhood is better. A well-planned neighborhood that considers the layout, street and block proportions and orientations, urban trees, and cooler materials can reduce the impacts of the

\* Corresponding author.

E-mail addresses: [msosa@mendoza-conicet.gob.ar](mailto:msosa@mendoza-conicet.gob.ar) (M.B. Sosa), [ecorrea@mendoza-conicet.gob.ar](mailto:ecorrea@mendoza-conicet.gob.ar) (E.N. Correa), [macanton@mendoza-conicet.gob.ar](mailto:macanton@mendoza-conicet.gob.ar) (M.A. Cantón).

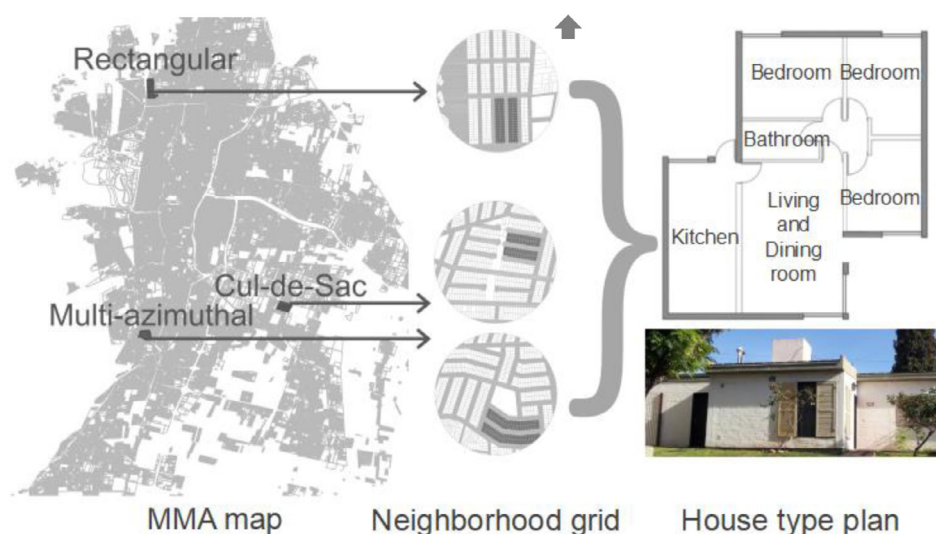


Fig. 1. Selected study sites: MMA location, neighborhood grid layouts, monitored streets, and house typology.

microclimate generated by the urban form [16,27,30,45]. While there is evidence that indicates that the urban form, or some of its attributes, affects energy demand, characterizing the effect of the urban form remains a major challenge [21,42,43]. The implications on operational energy use in buildings are not always explored, and there are few studies that have focused on this. Thus, it is important to evaluate how elements of the urban form affect building energy consumption [19]. Comprehensively understanding the relationship between urban form and energy use is important to formulate city-level climate change mitigation policies [23]. Rosenthal, Kinney, and Metzgerd [38] suggested that low-income neighborhoods should be prioritized in the climate adaptation planning of cities, and that disparities in accessing residential air conditioning are associated with heat-related mortality rates in New York. Therefore, socioeconomically weak communities are more vulnerable to the impacts of climate change [10,31,37,46]. Research in this area would aid the planning of energy-efficient social housing neighborhoods that considers microclimatic variables in the design stage.

### 1.1. Objectives

This study aims to:

- evaluate the impact of different social housing neighborhood designs on outdoor air temperatures and the energy consumption for cooling during summertime.
- improve energy efficiency at the neighborhood scale by providing planning and design strategies for social housing settlements in cities with arid climates.

## 2. Methodology

The following methodology was undertaken to conduct this study: (i) study site characterization and selection, (ii) microclimate monitoring, (iii) computational fluid dynamics (CFD) simulations, and (iv) estimation of energy consumption.

### 2.1. Study site characterization and selection process

This study was conducted in the Mendoza Metropolitan Area, Argentina (MMA), a region with a hot-dry climate (BSk) according to the Köppen Climate Classification. The MMA contains 62.8% of the population of Mendoza [13]. The energy demand faces a

Table 1

Features of the selected urban canyons.

Neighborhood grid	Multi-azimuthal	Cul-de-Sac	Rectangular
Street length (m)	255	145	192
Street width (m)	20	20	16
H/W	0.15	0.15	0.19
Street orientation	E-W	E-W	N-S
Sky view factor	0.69	0.57	0.35
Quantity of trees (u)	53	36	53
Tree species	<i>Morus alba</i>	<i>Ulmus umbraculifera</i>	<i>Morus alba</i>

maximum increase of 18% during the summer months (December and January). By relating the UHI and urban warming impacts to the energy demand for air conditioning, previous studies have observed an energy consumption increase of up to 20% in the MMA [7]. This is characterized by low building density, mainly constituting of single-family attached houses [14]. Currently, there is a housing deficit of 65 thousand homes in the MMA [53]. To improve the deficit, a National Housing Plan with two specific programs, “Social Housing” and “Housing=Work”, is being developed by the government. These housing programs provide the same house type regardless of context within the MMA, and no energy efficiency strategies have been considered (Fig. 1).

To select the most representative cases within the MMA, the study site selection process was categorized into three urban levels:

- Urban districts: The MMA contains six districts, namely, Mendoza Capital, Guaymallén, Las Heras, Godoy Cruz, Maipú, and Luján. The most populated districts were selected and they share borders with the Capital (Guaymallén: 16%, Las Heras: 12%, and Godoy Cruz: 11%). A graphic survey was conducted in the selected districts to identify the most representative urban block forms. The results of the survey show that 31% of the blocks in Godoy Cruz are rectangular, 48% in Guaymallén are irregular, and 33% of those in Las Heras are irregular while 30% are rectangular blocks with a North-South orientation. One neighborhood in each urban district was selected based on these results.
- Urban neighborhood: The selected neighborhoods have different layouts and block orientations but share some features that allow us to compare their microclimatic behaviors. For this study, urban neighborhoods with similar house types were selected to prevent the incidence of built-up characteristics. Ad-

**Table 2**  
Specifications of the measurement devices.

Device	Variable	Measurement range	Accuracy	Resolution
H08-003-02	Air temperature	−20 °C– +70 °C	± 0.7 °C at +21 °C	0.4 °C at +21 °C
S-LIB-M003	Solar radiation	0–1280 W/m <sup>2</sup>	± 10 W/m <sup>2</sup> or ± 5%	1.25 W/m <sup>2</sup>

ditionally, each neighborhood was classified and characterized according to a study by Stewart and Oke [48] and the Local Climate Temperature Zones for Urban Studies (LCZ). In Godoy Cruz, a multi-azimuthal grid neighborhood was selected (rectangular blocks with slight orientation changes). In Guaymallén, a Cul-de-Sac grid neighborhood was selected (irregular blocks and streets with one inlet/outlet, oriented E-W), and in Las Heras district, a rectangular grid neighborhood was selected (rectangular blocks oriented North-South). These three neighborhoods are forested and have equal low-density social housing typologies (i.e., second magnitude street trees, 16 and 20 m streets widths, 3 m house heights, and albedos of 0.2, 0.3, and 0.5 for the roofs, façades, and streets, respectively). According to the LCZ classification, the three study sites correspond to the open-low rise class with scattered trees subclass (LCZ 6b).

- Urban canyons: For monitoring the microclimate, one urban canyon was considered as representative and selected according to a characterization process that used a set of six indicators and descriptors, including street length, width, and orientation; the H/W ratio; sky view factor (SVF); and species and quantity of trees in the street. The SVF was calculated from hemispherical images that were captured with a Nikon® Coolpix digital camera equipped with a fisheye lens and then processed with Pixel de Cielo 1.0 software. The most predominant urban canyon in each studied neighborhood was selected due to its representative conditions. See Fig. 1 and Table 1.

## 2.2. Microclimate monitoring

Microclimatic data in the three urban canyons were captured during a 34-day measuring campaign (January 8 to February 10, 2014). A fixed sensor-type logger (H08-003-02; HOBO®; Cape Cod, MA) was installed 2 m from the ground in a solar radiation shield to prevent irradiation and ensure adequate air circulation [32]. The sensors recorded data every 15 minutes. January 18 was selected as the study day as the meteorological conditions were typical of a summer day in an arid region (high temperature, clear sky conditions, moderate wind, low relative humidity, and no precipitation) [55]. Additionally, a silicon pyrometer (S-LIB-M003; HOBO®; Cape Cod, MA) was mounted on a bracket in each canyon 2 m height above the ground. Sensors were positioned at the center of each urban canyon cross-section, which were mounted to a wooden mast on the sidewalks (for the E-W-oriented canyons, the mast was on the North side, and for the N-S-oriented canyons, the sensors were on the West side) (Fig. 2). The silicon pyranometer was mounted to the top of a bracket in an exposed spot to avoid shadowing. Table 2 shows the specifications of the measurement devices.

## 2.3. CFD simulations

ENVI-met software was used for this study, which is a 3D grid-based CFD tool for simulating surface-plant-air interactions using the fundamental laws of fluid dynamics and thermodynamics. It can be downloaded for free from <http://www.envi-met.com>. The use of this software has been widely validated by the academy [22,35,39,50].

ENVI-met requires two main input files, (i) the area input file, which contains the building layout, vegetation, soil type, receptors,

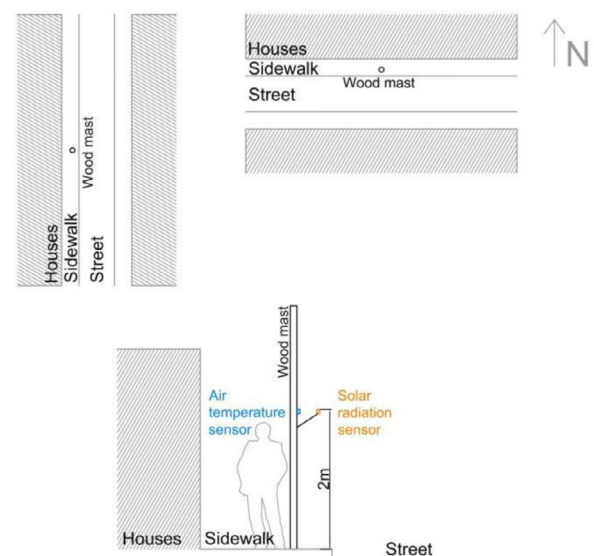


**Fig. 2.** Sensor positions in the monitored urban canyons.

and project location parameters, and (ii) the configuration file, containing simulation settings regarding the initialization values for meteorological parameters, definition of output folder names, and timings.

### 2.3.1. Scenario configuration and data validation

A total of 48 scenarios were generated in this study. Their designs follow the guidelines of the Mendoza Regulatory Law (4341/1978). Two street widths (16 and 20 m), one block length and width (100 m and 40 m, respectively), one building height (3 m), three neighborhood grids forms (multi-azimuthal, Cul-de-Sac, and rectangular), and four layout orientations (E-W, N-S, NE-SO and NW-SE) were used. Fig. 3 presents a graphical and quantified description of the urban scenarios, including the percentages and values of the built-up areas, impervious and pervious surfaces, H/W ratios, and SVF values for each case. The scenarios were simulated using ENVI-met 3.1 in two stages:

- Base cases: the first stage simulated the behavior of 24 scenarios that have no street trees and traditional albedos values ( $\alpha$  roofs 0.2,  $\alpha$  walls 0.3, and  $\alpha$  streets 0.5);
- Optimized cases: the second stage simulated 24 scenarios that have street trees and optimized albedos values ( $\alpha$  roofs 0.7,  $\alpha$  walls 0.3 and  $\alpha$  streets 0.5). The optimized albedos values follow the recommendations of a previous study conducted in the MMA [2]. The “Tb” model was selected from the ENVI-met PLANTS database to represent street trees, which was based on a field survey and observation of the vertical configurations of trees (a height of 10 m and LAD between 0.80 and 2.00 m<sup>2</sup>/m<sup>3</sup> were used for calculation).

The scenarios were modeled within a horizontal area of 258 × 258 m that comprised of 86 × 86 cell grids of 3 × 3 m. Each cell grid was 3 m in height, and there were 30 such grids (i.e., the spatial height of each model is 90 m). A total of seven receptors were used in each model: three were positioned along the urban

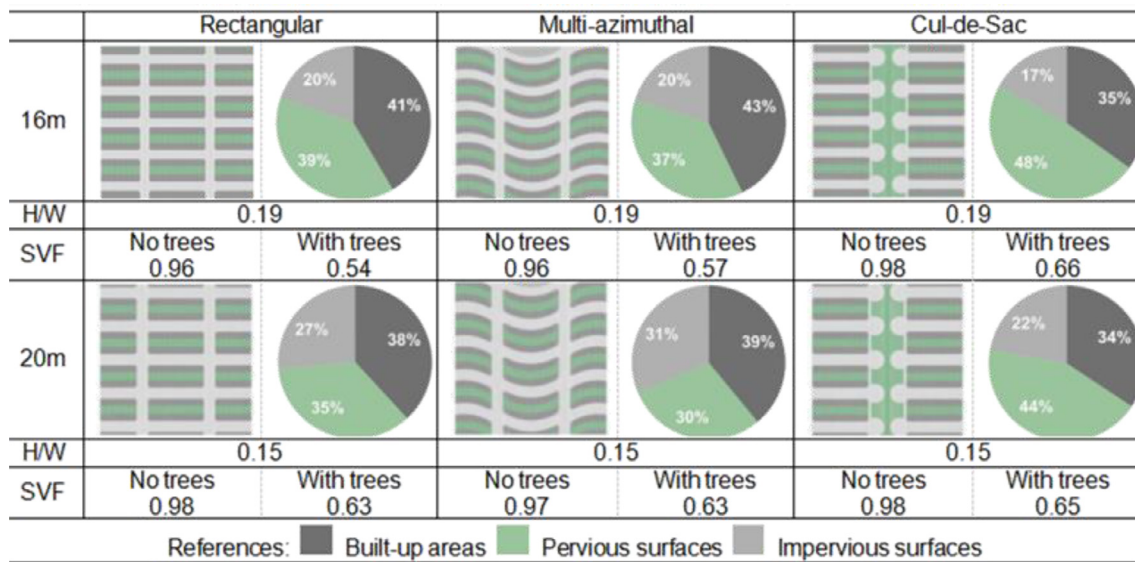


Fig. 3. Urban scenario characteristics.

Table 3

ENVI-met simulation input parameters. \* Default ENVI-met values.

ENVI-met input parameters after model adjustment	
<i>Meteorological</i>	
Mean wind speed 10 m from the ground (m/s, Airport meteorology station data)	2.5
Prevailing wind direction (Airport meteorology station data)	140°
Roughness length	0.1
Solar adjustment factor	1.3
Initial atmospheric temperature (K) (University of Wyoming, station 87418 Mendoza)	300
Specific humidity at 2500 m (g/kg <sup>-1</sup> )	2.8
Relative humidity at 2 m (%)	37
<i>Building</i>	
Indoor temperature (K)	297
Wall conductivity (W/m <sup>2</sup> K)	2
Roof conductivity (W/m <sup>2</sup> K)	0.78
Wall albedo	0.3
Roof albedo	0.2
<i>Soil</i>	
Initial upper soil layer (0–20 cm) temperature (K)	292
Initial upper soil layer (20–50 cm) temperature (K)	292
Initial deeper soil layer (below 50 cm) temperature (K)	290
Upper soil layer (0–20 cm) moisture content (%)	20
Upper soil layer (20–50 cm) moisture content (%)	35
Deeper soil layer (below 50 cm) moisture content (%)	60

canyon and the other four were located within the boundaries of the urban area. To ensure numerical stability and minimize boundary effects that may affect the output data, three (9 m) nesting grids were set around the main model area, as mentioned in previous ENVI-met modeling studies [20,29].

The predictions from the microclimatic simulations strongly depend on the initial boundary conditions and input data, therefore, care should be taken when defining the initial simulation parameters. In this study, the accuracy of the ENVI-met model was assessed by comparing the series of air temperature measurements from January 18, 2014 with the corresponding simulated values (see the input parameters in Table 3). The SVF values considered the adjustment of real case study values and those generated by the ENVI-met model.

The model was statistically evaluated using a set of recommended indices that describe the magnitude of the difference between the observation and prediction. The indices are: (i) the root mean square error, and the systematic and unsystematic root mean square error (RMSE, RSMES, and RSMEu, respectively), (ii) the mean absolute error (MAE), and (iii) the mean bias error (MBE).

The RMSE and MAE provide information on the average error and are suitable indicators of the model's performance. The MBE describes the direction of the error bias; its value is related to the magnitude of the values used. A negative MBE occurs when the predicted values are smaller than the observations. Based on statistical index values that were accepted in previous ENVI-met evaluation studies, the models can reliably simulate microclimates [6,51]. The adjustment values for the three models are shown in Fig. 4. The maximum, minimum, and average air temperatures, and the SVF values are presented and contrasted.

#### 2.4. Estimation of energy consumption

According to the study aims, we estimated the auxiliary energy demand ( $Q_{aux}$ ) for cooling houses under the 48 scenarios during the summer. The energy balance equations used give an initial approximation of the impact that the outdoor microclimate has on the indoor energy consumption Eq. (1) [45]. PREDISE freeware was used for this diagnostic phase (pre-design stage), which was developed by the INENCO research group of the Science department at



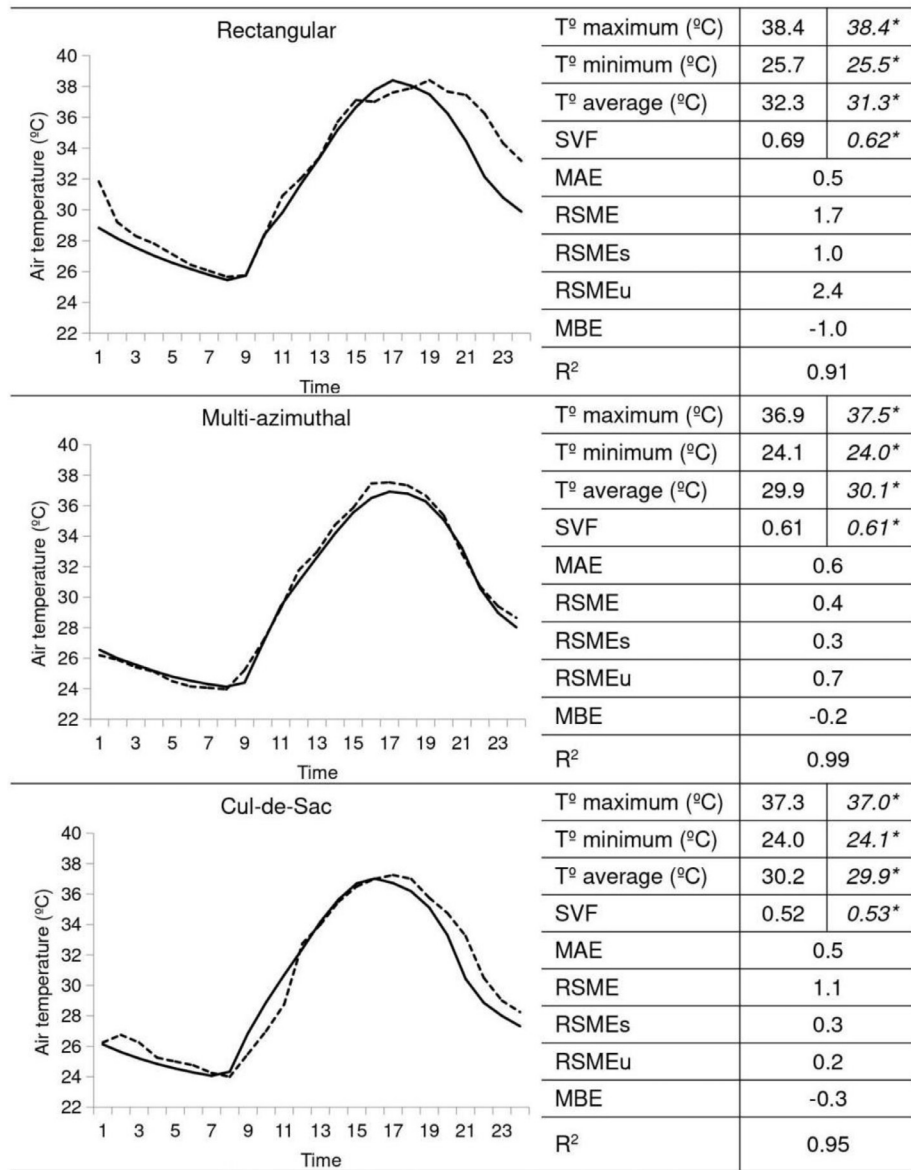


Fig. 4. Model adjustments, \*monitored values.

the National University of Salta, Argentina (<http://www.unsa.edu.ar/alejo/predise/>). PREDISE estimates the average indoor temperature and energy fluxes that the total volume of a building in a steady state exchanges with the environment through all its exposed surfaces within a short time period (immediate). This free-ware can also be used to support other detailed programs as it is independent from commercial applications. PREDISE estimates the  $Q_{aux}$  from the following energy balance equation:

$$CTU \times (T^{\circ}int - T^{\circ}ext) - Q_{solar} - Q_{gen} = Q_{aux} \quad (1)$$

where  $CTU$  is the heat load unit,  $T^{\circ}int$  is the average indoor temperature, which was set at 25 °C as suggested by the Argentinean Energy Department,  $T^{\circ}ext$  is the average exterior temperature obtained from the ENVI-met simulations,  $Q_{solar}$  is the direct solar gain through the windows, and  $Q_{gen}$  is the internal heat gain.

PREDISE requires a geographical, meteorological, building, and internal heat gain database to function. Geographical data indicates the study site (MMA), the meteorological data were obtained from the ENVI-met simulations results, the building data include the material characteristics of all exposed surfaces (roof, walls, win-

dows, and doors), and the internal heat gain data reflect the average consumption by the basic electrical and natural gas appliances of a four-person family household (one man, one woman, two children). The input parameters and values of the PREDISE database are presented in Table 4.

### 3. Results

#### 3.1. Outdoor thermal behavior

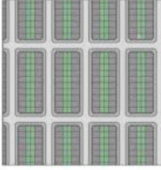
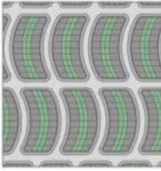
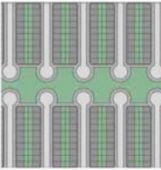
The results of the CFD simulations of the 48 scenarios (24 base and 24 optimized cases) are presented in Figs. 5 and 6. Fig. 5 is color coded from light blue (cool) to red (warm) based on the air temperature values, and the optimized and base cases are denoted as “opti.” and “base”, respectively.

From analyzing the thermal behaviors, we can see that:

- The optimized cases of all orientations and street widths are the coolest. The differences between the air temperatures of the optimized and base cases reach a maximum of 4.7 °C, minimum of 2.5 °C, and an average of 3.4 °C.

**Table 4**  
PREDISSE database parameters and values.

Geographical data	Latitude	−32.5
	Altitude (m.a.s.l)	746
	Albedo	0.2
Meteorological data	Maximum outdoor temperature (°C)	Defined by the CFD simulation results
	Average outdoor temperature (°C)	Defined by the CFD simulation results
	Horizontal solar radiation (MJ/m <sup>2</sup> )	Defined by the CFD simulation results
Building data	Building volume (m <sup>3</sup> )	240
	Building area (m <sup>2</sup> )	80
	Roof material	concrete slab
	Roof area (m <sup>2</sup> )	80
	Insulation	expanded polystyrene ( $\lambda = 0.03 \text{ W/m } ^\circ\text{C}$ of 0.10 m thick)
	Wall material	solid brick (0.20 m thick)
	Wall area (m <sup>2</sup> )	83
	Foundation perimeter (m)	41.2
	Door material	Wood
	Door area (m <sup>2</sup> )	2.2
	Total window area (m <sup>2</sup> )	9
	Windows per house	6
	Window azimuth	0°/ 45°/90°/135°/225°/180°/270°/315°
	Air infiltration (renovations per hour)	2
	Indoor comfort temperature (°C)	25
Internal heat gain	People (MJ/day)	29
	Electrical appliances (MJ/day)	8
	Natural gas appliances (MJ/day)	25

		N-S			NO-SE			E-O			NE-SO		
Scenario		O. C.	B. C.	$\Delta$	O. C.	B. C.	$\Delta$	O. C.	B. C.	$\Delta$	O. C.	B. C.	$\Delta$
 Rectangular	T <sup>o</sup> max. (°C)	37.5	42.0	-4.5	37.2	40.7	-3.5	37.7	42.2	-4.5	37.8	42.5	-4.7
	16 m T <sup>o</sup> min. (°C)	25.1	27.6	-2.4	25.8	28.1	-2.3	25.3	27.8	-2.5	25.8	27.8	-2.1
	T <sup>o</sup> ave. (°C)	30.6	33.9	-3.3	30.7	33.5	-2.9	31.0	34.4	-3.4	30.9	34.3	-3.4
	T <sup>o</sup> max. (°C)	38.1	42.1	-4.0	37.7	40.9	-3.1	38.3	42.3	-3.9	38.5	42.6	-4.1
	20 m T <sup>o</sup> min. (°C)	25.5	27.6	-2.1	26.2	28.1	-1.9	25.7	27.9	-2.2	26.0	27.9	-1.9
	T <sup>o</sup> ave. (°C)	31.1	34.0	-3.0	31.1	33.6	-2.5	31.5	34.4	-2.9	31.4	34.4	-3.0
 Multi-azimuthal	T <sup>o</sup> max. (°C)	37.7	41.5	-3.8	37.5	40.6	-3.1	37.7	41.8	-4.0	38.0	42.1	-4.1
	16 m T <sup>o</sup> min. (°C)	25.2	27.6	-2.3	25.8	28.0	-2.2	25.4	27.8	-2.3	25.9	27.7	-1.8
	T <sup>o</sup> ave. (°C)	30.8	33.7	-2.9	30.9	33.5	-2.6	31.0	34.1	-3.1	31.1	34.1	-3.0
	T <sup>o</sup> max. (°C)	38.0	41.7	-3.7	37.8	40.8	-2.9	38.1	41.9	-3.8	38.4	42.3	-3.9
	20 m T <sup>o</sup> min. (°C)	25.6	27.8	-2.2	26.2	28.1	-1.9	25.8	28.0	-2.2	26.1	27.9	-1.9
	T <sup>o</sup> ave. (°C)	31.1	33.9	-2.8	31.3	33.6	-2.4	31.4	34.3	-2.9	31.5	34.3	-2.8
 Cul-de-Sac	T <sup>o</sup> max. (°C)	38.3	41.9	-3.7	38.0	40.4	-2.4	38.3	41.8	-3.5	38.8	42.2	-3.4
	16 m T <sup>o</sup> min. (°C)	24.8	27.2	-2.4	26.1	27.9	-1.9	25.1	27.4	-2.3	25.5	27.5	-1.9
	T <sup>o</sup> ave. (°C)	30.7	33.7	-3.0	31.3	33.4	-2.1	31.1	34.1	-3.0	31.5	34.1	-2.6
	T <sup>o</sup> max. (°C)	38.3	41.8	-3.5	38.0	40.4	-2.4	38.4	42.0	-3.6	38.8	42.4	-3.6
	20 m T <sup>o</sup> min. (°C)	25.3	27.4	-2.1	26.3	28.0	-1.7	25.5	27.6	-2.1	26.0	27.7	-1.6
	T <sup>o</sup> ave. (°C)	30.9	33.8	-2.9	31.4	33.4	-2.0	31.3	34.2	-2.9	31.6	34.3	-2.6

**Fig. 5.** Air temperature values of the 48 urban scenarios. (For interpretation of the references to colour in this figure legend, the reader is referred to the web version of this article.)

- The NW-SE and N-S grid orientations are the coolest. In the NW-SE orientation, the maximum air temperatures are the coolest, the minimum temperatures of the N-S orientation are the coolest, and the average temperatures of both orientations are the coolest.
- The 16-m street width is the coolest in any orientation.
- The rectangular neighborhood grid is the coolest; 63% of the scenarios have maximum temperatures below 38 °C, 50% have minimum temperatures below 26 °C, and 31% have average temperatures lower than 31 °C. Regarding the multi-azimuthal

grid, 56% of the scenarios have maximum temperatures below 38 °C, 44% have minimum temperatures below 26 °C, and 25% have average temperatures below 31 °C. Finally, in the Cul-de-Sac grid, 13% of the scenarios have maximum temperatures below 38 °C, 38% have minimum temperatures below 26 °C, and 6% have average temperatures below 31 °C.

### 3.2. Energy consumption and neighborhood grid form

The influence of grid form on the energy consumption for cooling houses was quantified. Fig. 7 shows the net and percentage dif-

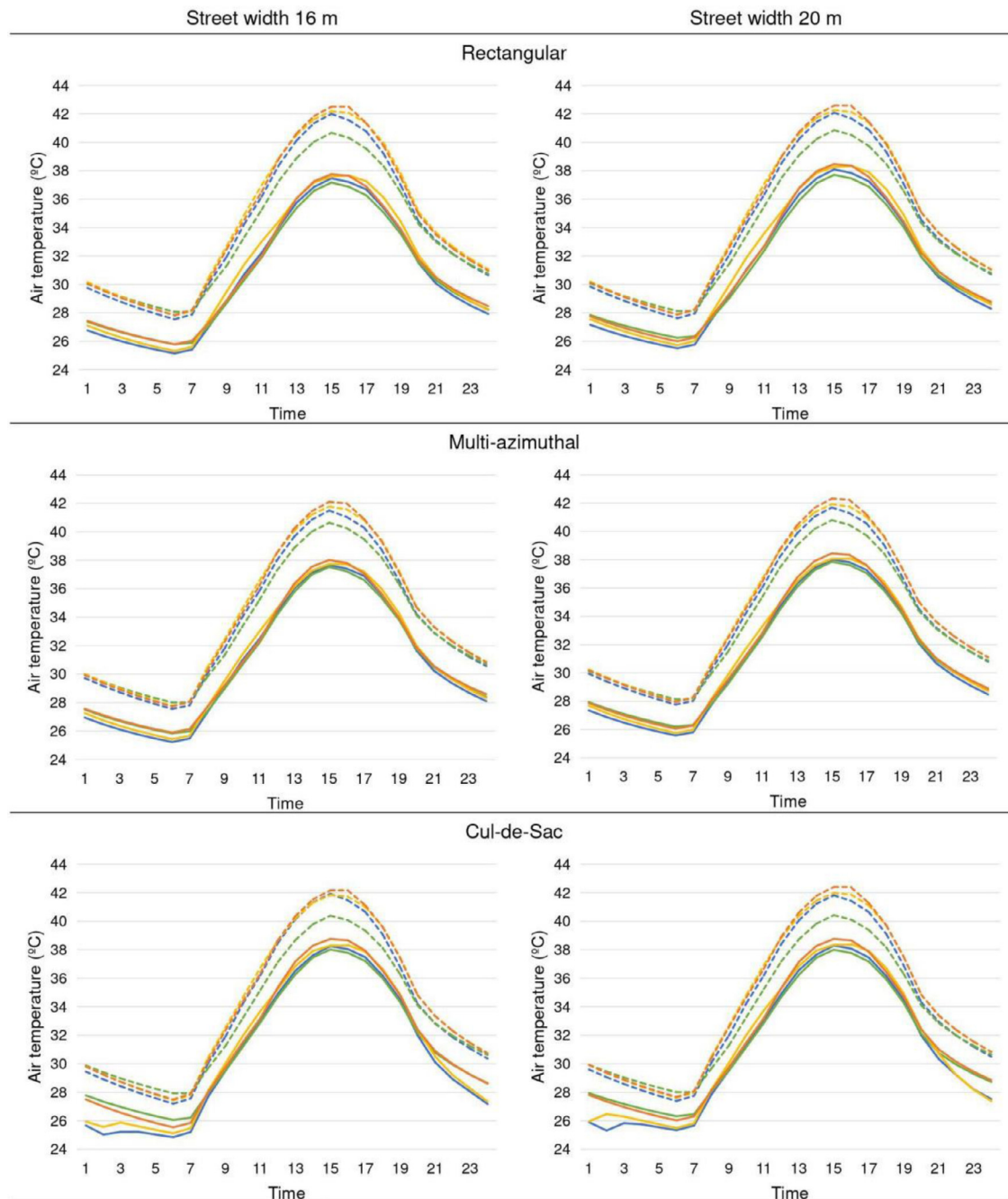


Fig. 6. Thermal behavior of the 48 urban scenarios.

ferences in energy consumption between the optimized and base cases scenarios. The table is divided according to the three urban characteristics: neighborhood grid, street width, and orientation. The Qaux values were estimated using PREDISE for maintaining the indoor temperature at 25 °C. The parameters and input values of the database are indicated in Table 4 (Section 2.4).

Regardless of the applied optimization strategies, i.e., albedo modification and urban trees, the results of the rectangular grid are as follows:

- The energy saving varies from 32 to 25%.
- The most efficient scenario is that with the 16 m street width and N-S orientation (179 kWh–2.2 kWh/m<sup>2</sup> for an 80 m<sup>2</sup> single-story attached house).

- The scenario with the greatest possibility of optimization in terms of its base conditions is that with the 20 m street width and E-W orientation (energy saving of  $\Delta 89$  kWh).

Analyzing the values of the multi-azimuthal grid shows that:

- The energy saving varies between 30 and 27%.
- The most efficient scenario is that with the 16-m street width and N-S orientation (184 kWh–2.3 kWh/m<sup>2</sup> for an 80 m<sup>2</sup> single-story attached house).
- The scenario with the greatest possibility of optimization in terms of its base conditions is that with the 16 m street width and E-W orientation (energy saving of  $\Delta 81$  kWh).

Analyzing the values of the Cul-de-Sac grid shows that:

- The energy saving varies between 30 and 21%.



Street width	Orientation	Rectangular grid				Multi-azimuthal grid				Cul-de-Sac grid			
		Optimized (kWh)	Base (kWh)	$\Delta$ (kWh)	%	Optimized (kWh)	Base (kWh)	$\Delta$ (kWh)	%	Optimized (kWh)	Base (kWh)	$\Delta$ (kWh)	%
16m	N-S	179	265	-86	32	184	260	-76	29	182	260	-78	30
	NO-SE	182	255	-73	29	187	255	-68	27	197	252	-55	22
	E-O	189	278	-89	32	189	270	-81	30	192	270	-78	29
	NE-SO	187	275	-88	32	192	270	-78	29	202	270	-68	25
20m	N-S	192	268	-76	28	192	265	-73	28	187	262	-75	29
	NO-SE	192	257	-65	25	192	265	-73	28	200	252	-52	21
	E-O	202	278	-76	27	200	275	-75	27	197	273	-76	28
	NE-SO	200	278	-78	28	202	275	-73	27	205	275	-70	25

Fig. 7. Cooling electricity consumption for one house compared between both scenarios.

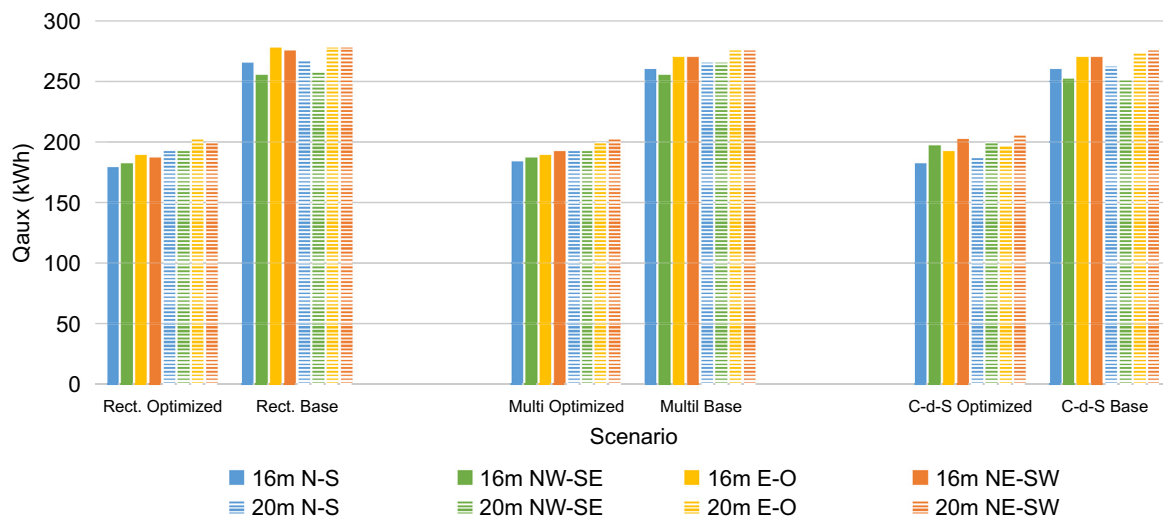


Fig. 8. Electricity consumption for cooling housing in both urban scenarios.

- The most efficient scenario is that with the 16 m street width and N-S orientation (182 kWh–2.2 kWh/m<sup>2</sup> for an 80 m<sup>2</sup> single story attached house).
- The scenario with the greatest possibility of optimization in terms of its base conditions is that with the 16 m street width and N-S and E-W orientations ( $\Delta$ 78 kWh of energy saving).

Fig. 8 shows and compares the energy efficiency of the optimized scenarios versus the base cases for each urban grid, street width, and orientation. The figure shows that grid orientation has a greater impact in the base cases (i.e., there were more differences in the  $Q_{aux}$  between orientations). The N-S grids are the most effective for the optimized cases, and the NW-SE grids are the most effective for the base cases.

### 3.3. Design strategies at neighborhood scale

Today, more than ever, environmental uncertainties are posing new challenges to cities and their communities, therefore, city management and planning regarding these uncertainties should be rethought [15]. A greater awareness of the need for policies that might eventually enhance resilience and reduce vulnerability to expected climate change impacts is needed for current settlements [54].

Urban planning recommendations and strategies based on the results obtained in this study are presented to improve the outdoor

thermal behavior of a low-density social housing neighborhood. The objective of these design and planning guidelines is to reduce the impact of the urban form on urban warming and the consequent increase in energy consumption. The urban design variables addressed were:

- Layout orientation: the N-S and NW-SE street orientations have the lowest air temperatures. The minimum air temperatures of the N-S and E-O orientations behave similarly, independent of the neighborhood grid.
- Built-up areas: the maximum air temperatures are lower in higher built-up areas. The multi-azimuthal grid form is recommended for areas with more built-up areas (43%) than the other two grid forms with the same urban areas (258 × 258 m).
- Impervious surfaces: air temperatures are lower in areas with less impervious surfaces. The Cul-de-Sac grid form is recommended as it has less impervious surfaces (17% versus 20%) than the other two grid forms.
- Pervious surfaces: air temperatures are lower in areas with more pervious surfaces. The Cul-de-Sac grid form is recommended as it has more pervious surfaces (48% versus 37 and 39% in 16 m streets width) than the other two grid forms. The rectangular grid form is recommended as it has similar percentages of pervious surfaces and built-up areas – when the street width is 16 m, this percentage is 40%.



- H/W ratio: this does not have a high relevance for low-density forested neighborhoods, as the outdoor thermal behavior can vary widely when the values of this indicator remain the same. The value of this indicator is relative to street width.
- SVF: at higher sky view factor values, the minimum air temperatures are lower. The recommended value of this indicator is in the order of 0.50, as this allows the incoming solar radiation to be reduced, improving nighttime release.
- Albedos: optimized albedo values ( $\alpha$  roofs 0.7,  $\alpha$  walls 0.3, and  $\alpha$  streets 0.5) can reduce maximum air temperatures more effectively. The incorporation of this strategy is recommended for horizontal surfaces (roofs, pavements, and sidewalks) and has a great impact on outdoor thermal behavior.
- Trees: street trees planted at regular distances with a homogeneous crown development allow easier regulation of solar exposure during the day and allows cooling at night. Deciduous second-magnitude species are recommended for low-density urban areas.

#### 4. Discussion

Stead and Marshall [47] argued that the literature has focused on macro features, such as settlement size, land use types, and density, while lower scale features, such as neighborhood design, may be relevant but have been overlooked. The optimization of the orientation of a single building has minimal reductions on annual energy use and cost, but, at a neighborhood-level, savings may be achieved by optimizing the orientation of a group of buildings [8,11,28,42,43]. Ko and Radke [19] found that the street configuration in Sacramento, California, has an important influence on household energy consumption, and it depends on the building's façade orientation. In this case, an E-W street orientation allows the construction more south-facing buildings. However, there can be variation in house orientation depending on the lot size and proportion, and house emplacement. For example, an E-W orientated lot (on a N-S street) can also accommodate a North or South-facing house if this house is not rigidly aligned to the lot boundary [18,26]. Therefore, the orientation of the street should be based on the area's latitude [41]. Ali-Toudert and Mayer [3] found that, in arid regions, it is difficult to shade an E-W street. In contrast, a N-S street provides enough shadow and creates a more pleasant microclimate. Therefore, for South regions in the southern hemisphere, this study recommends two neighborhood layout and street orientations (NW-SE and N-S) that are the most energy efficient during the season with the highest energy demand (i.e., summer). Regarding seasonal thermal behavior, Pearlmutter [33] suggested a residential neighborhood plan to improve thermal comfort conditions in Negev. The layout design considered the seasonally changing solar geometry, allowing shaded pedestrian walkways in the summer (2.5 m wide, most of which were aligned N-S) and solar access to buildings in the winter (main streets that provide vehicular access were generally oriented along an E-W axis).

Stone and Rodgers [49] recommends tree ordinances as policy strategies for mitigating the effects of urban development on regional climate change. Reducing the albedo of vertical surfaces and increasing the albedo of horizontal surfaces can also reduce outdoor air temperatures [1]. Middel, Chhetri, and Quay [27] demonstrated that a 25% increase in the tree canopy of residential neighborhoods resulted in an average decrease in temperature of 2.0 °C during the day, while cool roofs only reduced air temperature by 0.3 °C. Krayenhoff and Voogt [17] showed that an increase in the neighborhood albedo of 0.10 reduced the diurnal maximum air temperature by approximately 0.5 °C for a typical clear-sky mid-latitude summer day. Incorporating these two strategies in the MMA (street trees plus optimized albedos values) will reduce average air temperatures by 3.4 °C. This indicates that the incorporation

of street trees and suitable envelope materials into neighborhood design is vital for arid cities. Silva, Oliveira and Leal [42,43] recommend that rezoning more attached housing with higher density, incorporating more green space, and implementing incentives for appropriate tree planting can be effective tools for encouraging energy-efficient neighborhoods.

The aspects assessed in the international literature are congruent with the findings of this study. However, this study also evaluated the impact neighborhood grid form on energy consumption and air temperature, as well as layout orientation, forestation, and albedos. The rectangular grid is the most energy-efficient neighborhood form for low-density social housing neighborhood.

#### 5. Conclusions

Urban form and land use patterns significantly influence the thermal behavior and energy consumption of a city. As energy consumption is associated with average temperatures, we assessed how all strategies that aim to reduce the maximum or minimum temperatures would improve energy efficiency at the neighborhood scale. The results of changes in the thermal behavior of the 48 neighborhood scenarios in the MMA show that, with a suitable layout orientation, tree selection, and an improvement in the albedo of building materials, a traditional social house built without any bioclimatic design strategy would consume at least 21% less auxiliary energy for achieving a comfortable indoor temperature (25 °C) during the summer. This study also found that, with every 1 °C increase in average air temperature, the auxiliary energy consumption will increase by 26 kWh (0.3 kWh/m<sup>2</sup>). Similarly, within the three urban grids tested in the "optimized scenarios", there are differences in the energy consumption of 1–8% between orientations and street widths (i.e., neighborhoods with a 16 m street width orientated NW-SE in the rectangular grids consume 8% less energy than those with the same characteristics in the Cul-de-Sac grid). This observation highlights the importance of design and planning decisions in achieving more environmentally responsible and energy-efficient social housing settlements in cities with arid climates. Therefore, the results of this study present some implications for research and practice during the design of energy-efficient neighborhoods.

#### Acknowledgments

This work was supported by the *Agencia Nacional de Promoción Científica y Tecnológica* (ANPCYT) [grant number PICT 2011–0611]; and the *Consejo Nacional de Investigaciones Científicas y Técnicas* (CONICET) [grant number PIP 2011–00640].

#### References

- [1] N. Alchapar, C. Pezzuto, E. Correa, L. Labaki, The impact of different cooling strategies on urban air temperatures: the cases of Campinas, Brazil and Mendoza, Argentina, *Theor. Appl. Climatol.* 130 (2016) 35–50. <https://doi.org/10.1007/s00704-016-1851-5>.
- [2] N. Alchapar, E. Correa, in: *Comparison the Performance of Different Facade materials for Reducing Building Cooling needs. Eco-efficient materials for Mitigating Building Cooling Needs*, Woodhead Publishing, Cambridge, 2015, pp. 155–194.
- [3] F. Ali-Toudert, H. Mayer, Planning-oriented assessment of street thermal comfort in arid regions, in: *21th Conference on Passive and Low Energy Architecture*, Eindhoven, Netherlands, 2004, pp. 19–22.
- [4] C. Alonso, I. Oteiza, F. Martín-Consuegra, B. Frutos, Methodological proposal for monitoring energy refurbishment. Indoor environmental quality in two case studies of social housing in Madrid, Spain, *Energy Build.* 155 (2017) 492–502. <https://doi.org/10.1016/j.enbuild.2017.09.042>.
- [5] N. Baker, K. Steemers, *Energy and Environment in Architecture a Technical Design Guide*, Taylor & Francis, London, 2000 <http://dx.doi.org/10.4324/9780203223017>.
- [6] W.T. Chow, A.J. Brazel, Assessing xeriscaping as a sustainable heat island mitigation approach for a desert city, *Build. Environ.* 47 (2012) 170–181.

- [7] E. Correa, C. de Rosa, G. Lesino, Urban heat island effect on heating and cooling degree day's distribution in Mendoza's metropolitan area. Environmental costs, in: Proceedings of the 1st international conference on solar heating, cooling and buildings (EUROSUN 2008), 2, Curran associates, Inc, Red Hook, NY, USA, 2008, pp. 951–958.
- [8] A.V. Edminster, *Energy Free: Homes for a Small Planet*, Green Building Press, San Rafael, CA, 2009.
- [9] EIA, Independent statistics and analysis U.S. energy information and administration, 2016. [https://www.eia.gov/energyexplained/index.cfm?page=us\\_energy\\_homes](https://www.eia.gov/energyexplained/index.cfm?page=us_energy_homes).
- [10] S. Harlan, J. Decler-Barreto, W. Stefanov, D. Petitti, Neighborhood effects on heat deaths: social and environmental predictors of vulnerability in Maricopa county, Arizona, *Environ. Health Perspect.* 121 (2013) 197–204. <https://doi.org/10.1289/ehp.1104625>.
- [11] T.L. Hemsath, Housing orientation's effect on energy use in suburban developments, *Energy Build.* 122 (2016) 98–106. <https://doi.org/10.1016/j.enbuild.2016.04.018>.
- [12] IEA, International Energy Agency, WEO-2017 special report: energy access outlook, 2017. Download link [www.iea.org/publications/freepublications/publication/WEO2017SpecialReport\\_EnergyAccessOutlook.pdf](http://www.iea.org/publications/freepublications/publication/WEO2017SpecialReport_EnergyAccessOutlook.pdf).
- [13] INDEC, Instituto Nacional de Estadísticas y Censos, 2010. Censo nacional de población, hogares y viviendas. Argentina <http://www.censo2010.indec.gov.ar/>.
- [14] IPV, Instituto Provincial de la Vivienda de Mendoza (2010). Censo nacional de población, hogares y viviendas. Argentina. <http://www.censo2010.indec.gov.ar/>.
- [15] Y. Jabareen, Planning the resilient city: concepts and strategies for coping with climate change and environmental risk, *Cities* 31 (2013) 220–229. <https://doi.org/10.1016/j.cities.2012.05.004>.
- [16] S.K. Jusuf, N.H. Wong, E. Hagen, The influence of land use on the urban heat island in Singapore, *Habitat International* 31 (2007) 232–242, doi:10.1016/j.habitatint.2007.02.006.
- [17] E. Krayenhoff, J. Voogt, Impacts of urban albedo increase on local air temperature at daily–annual time scales: model results and synthesis of previous work, *J. Appl. Meteorol. Climatol.* 49 (2010) 1634–1648. <https://doi.org/10.1175/2010JAMC2356.1>.
- [18] Y. Ko, Urban form and residential energy use: a review of design principles and research findings, *J. Plann. Lit.* 28 (2013) 327–351. <https://doi.org/10.1177/0885412213491499>.
- [19] Y. Ko, J.D. Radke, The effect of urban form and residential cooling energy use in Sacramento, California, *Environ. Plann. B Plann. Des.* 41 (2014) 573–593. <http://dx.doi.org/10.1068/b12038p>.
- [20] F. Kong, C. Sun, F. Liu, H. Yin, F. Jiang, Y. Pu, G. Cavan, C. Skelhorn, A. Middel, I. Dronova, Energy saving potential of fragmented green spaces due to their temperature regulating ecosystem services in the summer, *Appl. Energy* 183 (2016) 1428–1440. <https://doi.org/10.1016/j.apenergy.2016.09.070>.
- [21] S. Lee, B. Lee, The influence of urban form on GHG emissions in the U.S. household sector, *Energy Policy* 68 (2014) 534–549.
- [22] C. Li, in: B. Huang (Ed.), GIS for Urban Energy Analysis, in Comprehensive Geographic Information Systems, Elsevier, Oxford, 2018, pp. 187–195. <https://doi.org/10.1016/B978-0-12-409548-9.09652-4>. ISBN 9780128047934.
- [23] C. Li, Y. Song, N. Kaza, Urban form and household electricity consumption: a multilevel study, *Energy Build.* 158 (2018) 181–193. <https://doi.org/10.1016/j.enbuild.2017.10.007>.
- [24] Y. Li, X. Zhao, An empirical study of the impact of human activity on long-term temperature change in China: a perspective from energy consumption, *J. Geophys. Res.* 117 (2012), doi:10.1029/2012JD018132.
- [25] T.P. Lin, A. Matzarakis, R.L. Hwand, Shading effect on long-term outdoor thermal comfort, *Build. Environ.* 45 (2011). 213–211 <http://dx.doi.org/10.1016/j.buildenv.2009.06.002>.
- [26] P. Littlefair, M. Santamouris, S. Alvarez, A. Dupagne, D. Hall, J. Teller, J. Coronel, N. Papanikolaou, *Environmental Site Layout Planning Solar Access, Microclimate and Passive Cooling in Urban Areas*, CRC, London, England, 2000.
- [27] A. Middel, N. Chhetri, R. Quay, Urban forestry and cool roofs: assessment of heat mitigation strategies in phoenix residential neighborhoods, *Urban for. Urban Greening* 14 (2015) 178–186. <https://doi.org/10.1016/j.ufug.2014.09.010>.
- [28] G. Mitchell, *Urban Development, Form and Energy Use in Buildings: A Review for the Solutions Project*, The University of Leeds, Leeds, UK, 2005.
- [29] T. Morakinyo, L. Kong, K. Lau, C. Yuan, E. Ng, A study on the impact of shadow-cast and tree species on in-canyon and neighborhood's thermal comfort, *Build. Environ.* 115 (2017) 1–17. <https://doi.org/10.1016/j.buildenv.2017.01.005>.
- [30] NRDC, Raimi + Associates and the Natural Resources Defense Council, 2011. A Citizen's Guide to LEED for Neighborhood Development: How to Tell if Development is Smart and Green. Download link [https://www.nrdc.org/sites/default/files/citizens\\_guide\\_LEED-ND.pdf](https://www.nrdc.org/sites/default/files/citizens_guide_LEED-ND.pdf).
- [31] R. Ojerio, C. Moseley, K. Lynn, N. Bania, Limited involvement of socially vulnerable populations in federal programs to mitigate wildfire risk in Arizona, *Nat. Hazards Rev.* 12 (2011) 28–36.
- [32] T.R. Oke, Initial Guidance to Obtain Representative Meteorological Observations at Urban Sites IOM Report No. 81, WMO/TD No. 1250, WMO, Geneva, 2004.
- [33] D. Pearlmutter, Patterns of sustainability in desert architecture, *Arid Lands Newsletter* 47 (2000) Desert Architecture for a New Millenium.
- [34] O. Preciado-Pérez, S. Fotios, Comprehensive cost-benefit analysis of energy efficiency in social housing. Case study: Northwest Mexico, *Energy Build.* 152 (2017) 279–289. <https://doi.org/10.1016/j.enbuild.2017.07.014>.
- [35] A. Qaid, H.B. Lamit, D.R. Ossen, R.N.R. Shahminan, Urban heat island and thermal comfort conditions at micro-climate scale in a tropical planned city, *Energy Build.* 133 (2016) 577–595. <https://doi.org/10.1016/j.enbuild.2016.10.006>.
- [36] J. Reyna, M. Chester, Energy efficiency to reduce residential electricity and natural gas use under climate change, *Nat. Commun.* 8 (2017). <https://doi.org/10.1038/ncomms14916>.
- [37] J. Rosenthal, E. Sclar, P. Kinney, K. Knowlton, R. Crauderueff, P. Brandt-Rauf, Links between the built environment, climate and population health: interdisciplinary environmental change research in New York city, *Ann. Acad. Med.* 36 (2007) 834–846.
- [38] J. Rosenthal, P. Kinney, K. Metzger, Intra-urban vulnerability to heat-related mortality in New York city, 1997–2006, *Health Place* 30 (2014) 45–60. <https://doi.org/10.1016/j.healthplace.2014.07.014>.
- [39] M. Roth, V.H. Lim, Evaluation of canopy-layer air and mean radiant temperature simulations by a microclimate model over a tropical residential neighbourhood, *Build. Environ.* 112 (2017) 177–189. <https://doi.org/10.1016/j.buildenv.2016.11.026>.
- [40] F. Salamanca, M. Georgescu, A. Mahalov, M. Moustauoui, M. Wang, Anthropogenic heating of the urban environment due to air conditioning, *J. Geophys. Res. Atmos.* 119 (2014) 1–17. <http://dx.doi.org/10.1002/2013jd021225>.
- [41] N. Shishegar, Street design and urban microclimate: analyzing the effects of street geometry and orientation on airflow and solar access in urban canyons, *J. Clean Energy Technol.* 1 (2013) 52–56. <http://dx.doi.org/10.7763/jocet.2013.v1.13>.
- [42] M. Silva, V. Oliveira, V. Leal, Urban form and energy demand: a review of energy-relevant urban attributes, *J. Plann. Lit.* 32 (2017) 346–365, doi:10.1177/0885412217706900.
- [43] M. Silva, V. Oliveira, V. Leal, Urban form and energy demand, *J. Plann. Lit.* (2017). <http://dx.doi.org/10.1177/0885412217706900>.
- [44] W. Solecki, C. Rosenzweig, L. Parshall, G. Pope, M. Clark, J. Cox, M. Wiencke, Mitigation of the heat island effect in urban New Jersey, *Global Environ. Change Part B* 6 (2005) 39–49, doi:10.1016/j.hazards.2004.12.002.
- [45] M.B. Sosa, E.N. Correa, M.A. Cantón, Urban grid forms as a strategy for reducing heat island effects in arid cities, *Sustainable Cities Soc.* 32 (2017) 547–556. <https://doi.org/10.1016/j.scs.2017.05.003>.
- [46] [46] Satterthwaite, D. (2008). Climate change and urbanization: effects and implications for urban governance. In Presented at UN expert group meet. popul. distrib., urban., intern. migr. dev. UN/POP/EGMURB/2008/16.
- [47] D. Stead, S. Marshall, The relationships between urban form and travel patterns: an international review and evaluation, *Eur. J. Transp. Infrastruct. Res.* 1 (2001) 113–141.
- [48] I.D. Stewart, T.R. Oke, Local climate zones for urban temperature studies, *B. Am. Meteorol. Soc.* 92 (2012) 1879–1900. <http://dx.doi.org/10.1175/bams-d-11-00019.1>.
- [49] B. Stone, M. Rodgers, Urban form and thermal efficiency: how the design of cities influences the urban heat island effect, *J. Am. Plann. Assoc.* 67 (2007) 186–198. <https://doi.org/10.1080/01944360108976228>.
- [50] S. Sun, X. Xu, Z. Lao, W. Liu, Z. Li, E. Higuera García, L. He, J. Zhu, Evaluating the impact of urban green space and landscape design parameters on thermal comfort in hot summer by numerical simulation, *Build. Environ.* 123 (2017) 277–288. <https://doi.org/10.1016/j.buildenv.2017.07.010>.
- [51] S. Tsoka, K. Tsikaloudaki, T. Theodosiou, Urban space's morphology and microclimatic analysis: a study for a typical urban district in the Mediterranean city of Thessaloniki, Greece, *Energy Build.* 156 (2017) 96–108. <https://doi.org/10.1016/j.enbuild.2017.09.066>.
- [52] UN-Habitat World Cities Report (2016). Urbanization and development: emerging futures.
- [53] [53] UNO Newspaper. (2017). Download link: [www.diariouno.com.ar/mendoza/en-mendoza-hay-un-deficit-habitacional-65-mil-viviendas-20171009-n1484644.html](http://www.diariouno.com.ar/mendoza/en-mendoza-hay-un-deficit-habitacional-65-mil-viviendas-20171009-n1484644.html).
- [54] P. Vellinga, N.A. Marinova, J.M. van Loon-Steensma, Adaptation to climate change: a framework for analysis with examples from the Netherlands, *Built Environ.* 35 (2009) 452–470.
- [55] [55] Weather Underground (2014). Retrieved from <https://espanol.wunderground.com/>.
- [56] J. Wong, L. Siu-Kit, From the 'urban heat island' to the 'green island'? A preliminary investigation into the potential of retrofitting green roofs in Mongkok district of Hong Kong, *Habitat Int.* 39 (2013) 25–35. <https://doi.org/10.1016/j.habitatint.2012.10.005>.
- [57] C. Zhao, G. Fu, X. Liu, F. Fu, Urban planning indicators, morphology and climate indicators: a case study for a north-south transect of Beijing, China, *Build. Environ.* 46 (2011) 1174–1183. <https://doi.org/10.1016/j.buildenv.2010.12.009>.